Preparation of Diamond Films in a Low Pressure Inductively Coupled RF Plasma

Katsuyuki Okada, Shojiro Komatsu, Takamasa Ishigaki, and Seiichiro Matsumoto

National Institute for Research in Inorganic Materials
1-1 Namiki, Tsukuba, Ibaraki 305, Japan

Abstract

A 13.56 MHz low pressure inductively coupled plasma(ICP) system has been applied to prepare diamond films from a $CH_4/H_2/Ar$ plasma. The morphology of the resultant deposit was scale-like, and crystal facets were not clearly seen. Although the deposit became sparse as the flow rate of Ar([Ar]) increased, it recovered dense and the grain size became small with further increase of [Ar]. In the Raman spectra, the relative intensity of the peak around 1580 cm^{-1} to that of the peak around 1355 cm^{-1} became strong as the [Ar] increased.

1.Introduction

Recent plasma dry processes require wide area and high density plasma at low pressures. An electron cyclotron resonance(ECR) plasma was first developed to meet these conditions. Subsequently, a helicon-wave excited plasma was developed. It has been recently found[1] that the density of an inductively coupled plasma(ICP) becomes high at low pressures(<1 Torr). It is reported[2] that the plasma density after the transition from a low density E-discharge to a high density H-discharge reaches $\sim 10^{12} cm^{-3}$. It is necessary in plasma-enhanced chemical vapor deposition(PE-CVD) to get a sufficient radical flux for deposition. Thus the ICP is thought to be an expected method for PE-CVD at low pressures.

A microwave plasma and an ECR plasma have been generally used for the synthesis of diamond films by PE-CVD, while there was a few report on RF plasma CVD[3-5]. Typical deposition pressures were order of 10 Torr in those experiments. In this study, a 13.56 MHz low pressure ICP system has been utilized as a radical source, and applied to prepare diamond films from a $CH_4/H_2/Ar$ plasma.

2.Experiment

The plasma torch designed in this study was modeled on the collimated

plasma beam reactor[6]. The schematic view of the plasma reactor system is illustrated in Fig.1. It consisted of a water-cooled quartz tube surrounded with a teflon tube placed at the bottom of a stainless-steel chamber. A plasma beam was generated by an aperture made of BN at the bottom of the chamber. In the gas inlet system, sheath gas was introduced to flow fast along the quartz tube wall, while source gas was admitted along the central axis of the reactor. The chamber was pre-evacuated below 3×10^{-5} Torr by a turbo molecular pump(200 l/sec). An electrostatic shield(Faraday shield)[1,7] was placed between the RF coil and the quartz tube to rule out the electrostatic coupling from RF coil to plasmas. The quartz tube was wrapped with a grounded copper plate slitted at regular intervals along the azimuthal direction. The substrate holder was manipulated from the top of the chamber. Molybdenum plates and silicon (100) wafers(ϕ 10 mm) were used as a substrate. The substrate was heated by a tungsten filament. The substrate temperature(Ts) was monitored with a sheathed thermocouple, and kept at a prescribed temperature within ± 1℃ by a proportional integral derivative(PID) controller.

The deposition conditions were as follows. The input plasma power was 1 kW. The flow rates of $CH_4/H_2/Ar$ were 1.5/50/0-28 sccm, respectively. The total pressure(Pr) varied from 12 to 33 mTorr. The Ts was kept at 920 ℃. The deposition time was 1 hour.

3.Results and discussion

It is known[1,7] that the electrostatic(capacitive) coupling from RF coil to plasmas in the ICP brings about contaminations due to the etching of the quartz tube. We have previously reported[8] that Faraday shield rules out the electrostatic coupling and suppresses the etching of the quartz tube.

Fig.2 shows the SEM micrographs of the resultant deposits. The deposition conditions were same except for the flow rate of Ar([Ar]). Fig.2 (a), (b), (c), and (d) correspond to [Ar]=0, 7, 14, and 28 sccm, respectively. In Fig.2(a), the morphology of the deposit was scale-like, and crystal facets were not clearly seen. The morphology of Fig.2(b) was similar to that of Fig.2(b). As the [Ar] increased, the deposit became sparse in Fig.2(c). However, the deposit recovered dense and the grain size became small in Fig.2(d) in case of the further increase of [Ar].

Fig.3 presents the Raman spectra corresponding to the Fig.2. In each spectrum, two peaks around 1355 cm^{-1} and 1580 cm^{-1} appeared. The peak around 1580 cm^{-1} is assigned to graphite, and the peak around 1355 cm^{-1} to disordered microcrystalline graphite. The peak due to diamond at 1333 cm^{-1} was not clearly identified because the crystal size was small and/or the diamond peak was overlapped by the peak of disordered graphite. In our previous report[8], the

resultant deposits prepared in a similar condition were identified as diamond crystallites by TEM and RHEED. As the [Ar] increased, the relative intensity of the peak around 1580 cm^{-1} to that of the peak around 1355 cm^{-1} became strong.

The main excitation processes in methane plasmas and their theoretical activation energies are listed below[9].

$CH_4 + e \rightarrow CH(A^2\Delta) + H_2 + H + e$ $\quad E_{th} = 12.2$ eV (1)

$CH_4 + e \rightarrow CH_3 + H(n=4) + e$ $\quad E_{th} = 17.1$ eV (2)

$CH_4 + e \rightarrow CH_2 + H_2(G^1\Sigma_g^+) + e$ $\quad E_{th} = 19$ eV (3)

$H_2 + e \rightarrow H(n=4) + H + e$ $\quad E_{th} = 17$ eV (4)

$H + e \rightarrow H(n=4) + e$ $\quad E_{th} = 12.75$ eV (5)

On the other hand, the energy threshold of the 750.4 nm emission line of Ar is 13.5 eV, thus its energy dependence is similar to that of the CH and H.It is therefore expected that CH and H radicals increase with the addition of Ar. These changes of radical products are thought to affect the morphologies of the resultant deposits.

Acknowledgement

The authors would like to thank Mr. M.Tsutsumi for the SEM observations.

References

[1]J.Hopwood, Plasma Sources Sci. Technol. **1**, 109(1992).
[2]J.Amorim, H.S.Maciel, and J.P.Sudano, J. Vac. Sci. Technol. **B9**, 362(1991).
[3]S.Matsumoto, J. Mater. Sci. Lett. **4**, 600(1985).
[4]S.Mitura, J. Cryst. Growth **80**, 417(1987).
[5]D.E.Meyer, R.O.Dillon, and J.A.Woollam, J. Vac. Sci. Technol. **A7**, 2325(1989).
[6]S.Komatsu, Y.Moriyoshi, M.Kasamatsu, and K.Yamada, J. Appl. Phys. **70**, 7078(1991)
[7]Y.Hikosaka, M.Nakamura, and H.Sugai, Jpn. J. Appl. Phys. **33**, 2157(1994).
[8]K.Okada, S.Komatsu, T.Ishigaki, and S.Matsumoto, The Proceedings of 1994 MRS Fall Meeting.
[9]A.Pastol and Y.Catherine, J. Phys. D: Appl. Phys. **23**, 799(1990).

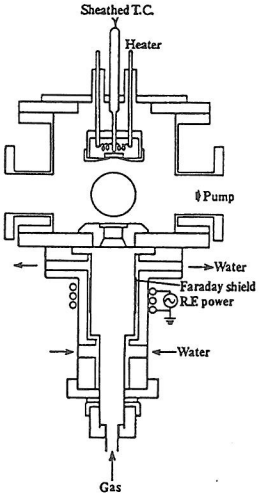

Fig. 1 Schematic diagram of the ICP reactor system.

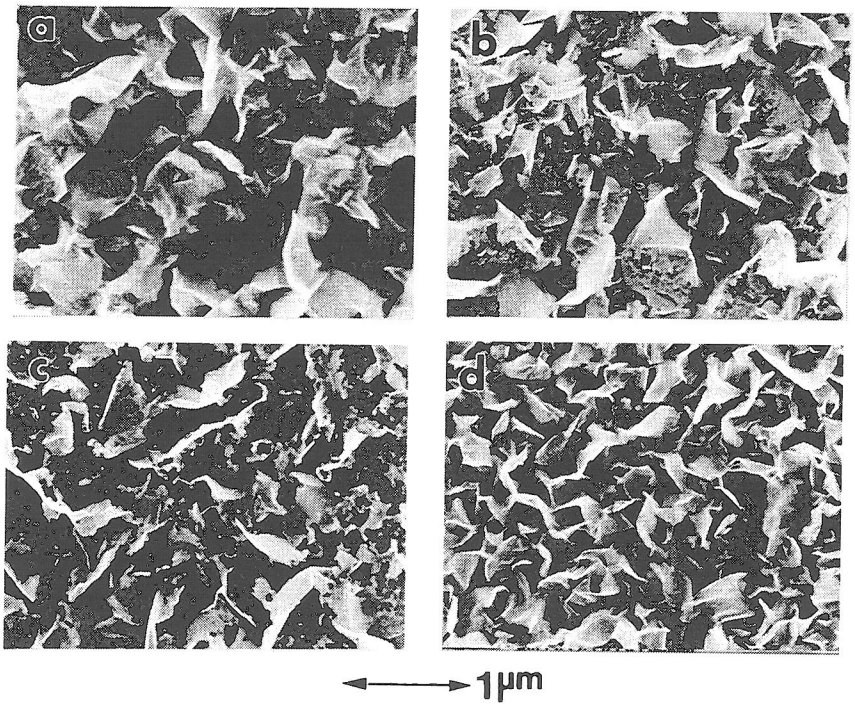

Fig.2 SEM micrographs of the obtained deposits; (a) [Ar]=0 sccm, (b) [Ar]=7 sccm, (c) [Ar]=14 sccm, and (d) [Ar]=28 sccm, respectively.

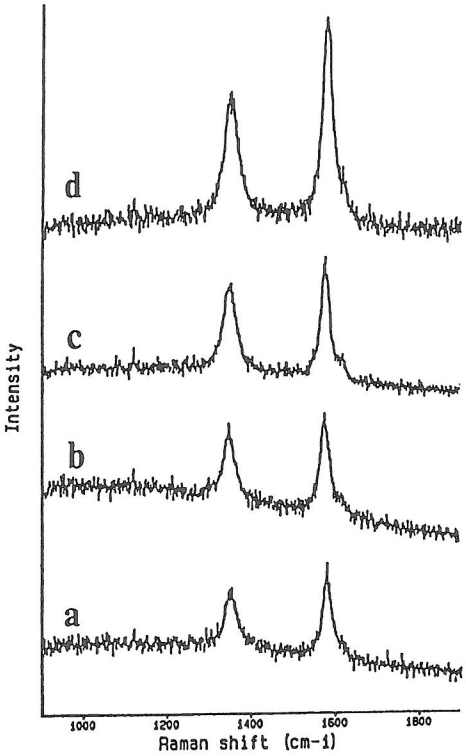

Fig.3 Raman spectra of the obtained deposits corresponding to Fig.2.